Ultrafast Enhancement of Ferromagnetism via Photoexcited Holes in GaMnAs

J. Wang,[1] I. Cotoros,[1] K. M. Dani,[1] X. Liu,[2] J. K. Furdyna,[2] and D. S. Chemla[1]

[1]*Materials Sciences Division, Lawrence Berkeley National Laboratory and Department of Physics, University of California at Berkeley, Berkeley, California 94720, USA*

[2]*Department of Physics, University of Notre Dame, Notre Dame, Indiana 46556, USA*

(Received 17 February 2007; published 22 May 2007)

We report on the observation of ultrafast photoenhanced ferromagnetism in GaMnAs. It is manifested as a transient magnetization increase on a 100 ps time scale, after an initial subpicosecond demagnetization. The dynamic magnetization enhancement exhibits a maximum below the Curie temperature T_c and dominates the demagnetization component when approaching T_c. We attribute the observed ultrafast collective ordering to the *p-d* exchange interaction between photoexcited holes and Mn spins, leading to a correlation-induced peak around 20 K and a transient increase in T_c.

DOI: 10.1103/PhysRevLett.98.217401 PACS numbers: 78.20.Jq, 42.50.Md, 78.30.Fs

There has been long and intense interest in searching for possibilities of ultrafast enhancement of collective magnetic order via photoexcitation. Such photoexcitation would lead to fascinating opportunities both for establishing a transient cooperative phase from an uncorrelated ground state and for determining the relevant time scales for the buildup of order parameters. Previous time-resolved investigations in paramagnetic II–VI semiconductors provided evidence for collective photoexcitations that led to the formation of magnetic polarons [1]. Substantial recent progress has been made in observing ultrafast spin reorientation, e.g., in antiferromagnetic materials [2,3]. However, most prior experiments in magnetically ordered materials only show an ultrafast decrease of the magnetization amplitude due to laser induced electronic heating [4]. Recently, several experiments in strongly correlated manganites and transition metal alloys revealed transient photoinduced magnetization on ultrafast time scales, but only demagnetization could be seen at temperatures away from T_c. The role of ultrafast pumping is most likely a thermal perturbation of competing phases near critical points [5,6].

The discovery of hole-mediated ferromagnetism in III–V ferromagnetic semiconductors (III–V FMSs) such as GaMnAs and InMnAs [7] offers unique opportunities and flexibility for nonthermal control of magnetism. Unlike other types of magnets, the ferromagnetic exchange between localized Mn moments is mediated by free hole spins through *p-d* interaction $H_{p\text{-}d} \sim J_{pd}\mathbf{S}\cdot\mathbf{s}$ ($J_{pd} \sim$ 1 eV), making the magnetic properties a sensitive function of the hole density. For instance, the trend of experimental T_c in GaMnAs is shown to be proportional to $p^{1/3}J_{pd}^2$, for a wide range of hole densities p [8]. Recently, hole-density-tuning via external stimuli such as cw light excitation [9] and electrical gating [10] has demonstrated clear enhancement of magnetization and increase of T_c, as illustrated in Fig. 1(a). However, no time-resolved experiments in III–V FMSs have shown transient photoinduced magnetization, and the time scale for the enhancement of collective order is completely unknown. So far only ultrafast demagnetization and quenching dynamics were observed, due in part to the relatively high pump fluences used (~1 mJ/cm^2) [11,12]. Moreover, recent theory has pointed to the critical role of the Mn-hole exchange correlation in ultrafast, nonthermal manipulation of magnetization in GaMnAs [13], but no experimental evidence for this has been reported. In addition to their fundamental scientific interest, III–V FMSs are among the most promising candidates for future "multifunctional" devices and for quantum information

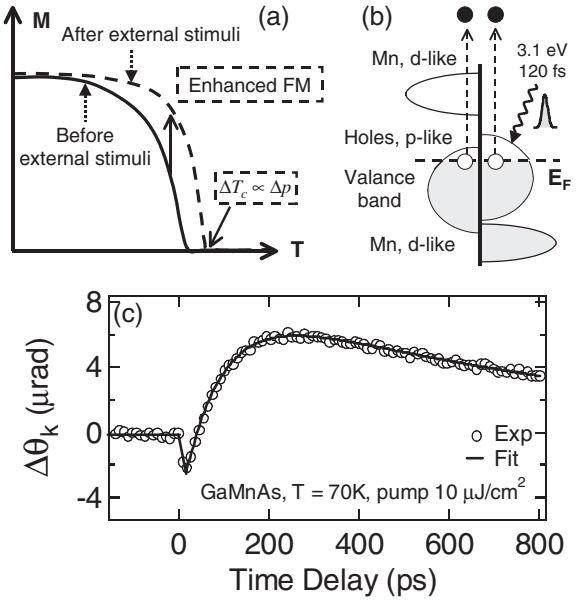

FIG. 1. (a) Illustration of hole-density-tuning effects via external stimuli in III–V FMSs seen in the static experiments [9,10]. FM: ferromagnetism. $\triangle p$ is hole density change. (b) Schematic diagram of the spin-dependent density of states in GaMnAs. Femtosecond pump pulses create a transient population of holes in the valence band. (c) Time-resolved MOKE dynamics at 70 K and under 1.0 T field. Transient enhancement of magnetization, with ~100 ps rise time, is clearly seen after initial fast demagnetization. Thick line is the fit described later in the text.

technology based on the spin degree of freedom [14]. It is thus of significance to explore ferromagnetic enhancement in III–V FMSs on technologically important, subnanosecond time scales.

In this Letter, we report the observation of ultrafast enhancement of ferromagnetism in GaMnAs. Our data clearly show photoinduced magnetization on a 100 ps time scale after initial subpicosend demagnetization. The dynamic magnetization enhancement exhibits a maximum below T_c and dominates the demagnetization component when approaching T_c. Our analysis and theoretical simulations based on the $H_{p\text{-}d}$ interaction between photoexcited holes and Mn spins explain the salient features of the experiment showing, in particular, a correlation-induced peak around 20 K and a transient increase in T_c.

The sample studied in the present work was a GaMnAs/GaAs heterostructure with a Curie temperature of 77 K. The sample was grown by low-temperature molecular beam epitaxy (MBE) and consisted of a 73 nm $Ga_{0.925}Mn_{0.075}As$ layer deposited on a GaAs buffer layer and a semi-insulating GaAs (100) substrate. The background hole density was approximately 3×10^{20} cm^{-3}. Our measurements involved ultraviolet pump and near-infrared probe magneto-optical Kerr effect (MOKE) spectroscopy. The experimental setup consisted of a femtosecond oscillator with 120 fs pulse duration and a β-BaB_2O_4 (BBO) crystal in the pump path for doubling the photon energy. The pump beam was at 3.1 eV and was linearly polarized, with peak fluences $\simeq 10\ \mu J/cm^2$. Figure 1(b) illustrates that femtosecond pump pulses create a large density of holes in the valence band of GaMnAs. A small fraction of the fundamental beam at 1.55 eV was used as a probe, detecting magnetization via the polar MOKE angle θ_K [15]. The low pump peak fluences and the high pump photon energy minimize spurious effects such as two-photon absorption and pump scattering. Additionally, the "magnetic origin" of the transient MOKE response is confirmed by separate measurements showing the overlap of the pump-induced rotation and ellipticity through the entire time scan range [16].

A typical temporal profile of transient MOKE changes $\Delta\theta_K$ at 70 K is shown in Fig. 1(c), with a field of 1.0 T perpendicular to the sample surface to align the magnetization. Two mutually competing dynamic magnetization processes are observed: an initial subpicosecond demagnetization ($\Delta\theta_K < 0$), followed by a distinct magnetization rise on a 100 ps time scale ($\Delta\theta_K > 0$). The two processes show different temperature dependences, as shown in Figs. 2(a) and 2(b). At elevated lattice temperature, the 200 fs demagnetization components [inset of Fig. 2(b)] quickly diminish and nearly disappear above T_c. This is also seen in the 600 fs and 3 ps traces in Fig. 2(c). More intriguingly, an enhancement of the transient magnetization begins to dominate the demagnetization component at high temperatures. The temporal traces of $\Delta\theta_K$ at temperatures from 40 to 70 K in Fig. 2(b) clearly show that the net

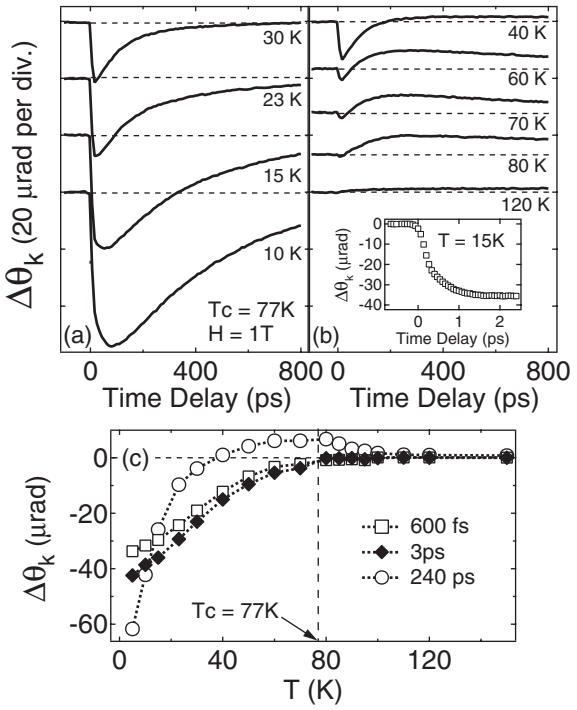

FIG. 2. (a),(b) Temporal traces of photoinduced magnetization changes at different temperatures. All traces are intentionally offset for clarity. Inset: the first 2 ps demagnetization dynamics at 15 K. (c) Temperature dependence of magnetization changes at different time delays—600 fs (squares), 3 ps (diamonds) and 240 ps (circles), respectively.

magnetization changes become positive at long time delays. Figure 2(c) summarizes the photoinduced magnetization changes at 240 ps revealing $\Delta\theta_K > 0$ above 40 K. The photoinduced magnetization persists above T_c—as is clearly visible in the 80 K trace [Fig. 2(b)]—and gradually vanishes at higher temperatures.

MOKE signals, measured with the 1.55 eV probe, arise from the macroscopic magnetization $\mathbf{M}$—average localized Mn spins—through the coupling of the spin-split electronic states near the band edge. The background carrier spin contribution to $\mathbf{M}$ is negligible, and photoexcited transient carriers are not spin polarized since the pump contains no net angular momentum. Thus the positive MOKE signals, rising on a 100 ps time scale, clearly indicate an ultrafast alignment of Mn spins and an enhancement of ferromagnetic order. Our results reveal the ultrafast time scale of this process, not accessible in previous static measurements [9,10].

We attribute the observed ultrafast photoenhanced ferromagnetism to the transient hole-Mn interaction via the $H_{p\text{-}d}$ exchange, as follows. At early pump-probe delays ($\triangle t \sim 0$ fs), the ultrashort laser pulses generate a nonequilibrium distribution of spin-unpolarized electron-hole pairs in GaMnAs under a finite external H field. During the first picosecond ($\triangle t < 1$ ps), the photoexcited hot holes will experience efficient spin-flip scattering with the localized Mn moments, manifesting this as a subpicosecond demagneti-

zation component. This results from the off-diagonal elements of the exchange Hamiltonian $H_{p\text{-}d}$ ($\sim J_{pd}\mathbf{S}_{\pm}\cdot\mathbf{s}_{\mp}$), which cause the spin polarization of the Mn ions to transfer to the holes within several hundred femtoseconds, similar to the femtosecond demagnetization first reported in InMnAs [11]. Meanwhile, the hot hole distribution quickly loses its energy via carrier-phonon scattering (optical phonon energy ~36 meV), resulting in a rapid termination of demagnetization (within the first picosecond). At longer pump-probe delays of $\triangle t > 1$ ps, the photoexcited, thermalized holes, settling down in the spin-split bands, can now participate in the process of hole-mediated ferromagnetic ordering. These extra holes enhance the Mn-Mn exchange correlation and polarize Mn spins via the mean-field (diagonal) elements of the exchange Hamiltonian $H_{p\text{-}d}$ ($\sim J_{pd}\mathbf{S}_z\cdot\mathbf{s}_z$), thereby increasing the macroscopic magnetization.

In order to elucidate the salient features of the photoenhanced ferromagnetism, we decompose the transient MOKE changes shown in Fig. 2 into demagnetization ($-\triangle\theta_k^d$) and enhanced magnetization ($\triangle\theta_k^m$) components, based on their different time scales. The temporal profile of $\triangle\theta_k$ is well described by $\triangle\theta_k^d \exp(-t/\tau_d) + \triangle\theta_k^m[1-\exp(-t/\tau_m)]\exp(-t/\tau_c)$. Here $-\triangle\theta_k^d$ and τ_d in the first term are the magnitude of demagnetization and the recovery time determined by the slow heat diffusion process, respectively. In the second term, $\triangle\theta_k^m$ and τ_m are the magnitude and buildup time of the enhanced magnetization component, respectively, while τ_c accounts for the final decay of the magnetization enhancement via hole diffusion and recombination. The time constant τ_c is on the order of a few nanoseconds, as seen in the decay of the positive MOKE signal. As an example, the thick line in Fig. 1(c) represents the fit of the MOKE dynamics at 70 K.

Figure 3 plots the temperature dependence of $-\triangle\theta_k^d$ and $\triangle\theta_k^m$. The $-\triangle\theta_k^d$ profile resembles the static magnetization curve of the sample [inset of Fig. 3(a)], exhibiting strong deviation from the classical mean-field convex shape. This nonclassical behavior of magnetization arises from the existence of two strongly interacting spin ensembles, Mn and holes, as discussed in [17]. More intriguingly, the magnetization enhancement $\triangle\theta_k^m$ in Fig. 3(b) shows a distinctly different temperature profile, with a peak of ~0.5% of the saturation magnetization M_0 around 20 K (static θ_k at 5 K ~4 mrad) and a prolonged tail extended to ~120 K. The extended profile beyond T_c is expected as the combined effect of an applied external field of 1.0 T and of hole-enhanced magnetic susceptibility in the paramagnetic state. The most salient feature of the photoenhanced ferromagnetism is the peak near 20 K, which is a manifestation of the Mn-hole correlation $H_{p\text{-}d}$.

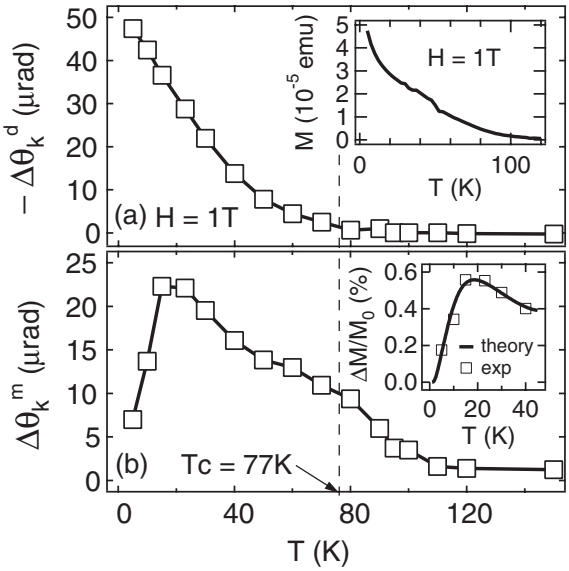

FIG. 3. Decomposed demagnetization $-\triangle\theta_k^d$ (a) and enhanced magnetization $\triangle\theta_k^m$ (b) components are plotted as a function of temperature. The static magnetization curve under 1.0 T field is shown as the inset in (a). The simulation $\triangle M/M_0$ (thick line, $\triangle T_c = 1.1$ K and the hole-Mn ratio of 0.06) and experimental values (circles, normalized by static θ_k at 5 K) of the photoenhancement peak ~20 K are shown as the inset of (b).

This can be qualitatively understood as follows: the ferromagnetic molecular field acting on the Mn ions (holes) is determined by the average spin polarizations of the holes (Mn ions) via the Mn-hole exchange coupling J_{pd}. The effective field acting on the holes is much larger than that acting on the Mn ions, because of the large density of Mn ions compared to the holes. As a consequence, the hole polarization will remain saturated at a temperature T_h much higher than that needed for saturating the Mn magnetization ($T_{\mathrm{Mn}} \sim 0$). As the lattice temperature increases above T_{Mn} but less than T_h, the Mn spins with partial alignment begin to be efficiently polarized via photoexcited holes with near-unity magnetization. However, as the lattice temperature rises higher than T_h, because of reduced hole polarization the efficiency of this magnetization enhancement process quickly drops, thus resulting in a magnetization enhancement maximum at some temperature on the order of T_h.

Next we present a simple theoretical calculation to simulate the Mn-hole correlation-induced peak around 20 K. As we discussed, the hole-enhanced ferromagnetic correlation results in an increase of T_c ($\triangle T_c > 0$). We calculate the experimental nonclassical magnetization curve [inset of Fig. 3(a)] based on a modified Weiss mean-field model to take into account the $H_{p\text{-}d}$ correlation [17]:

$$M(T,\Delta T_c)/M_0 = B_S\left\{-3\frac{T_c+\Delta T_c}{T}\gamma S^* B_s\left[-3\frac{T_c+\Delta T_c}{T}\gamma^{-1}S^*\frac{M(T,\Delta T_c)}{M_0}+\frac{g_h\mu_B H}{k_B T}\right]-\frac{g_i\mu_B H}{k_B T}\right\},$$

where $B_{S,s}(x)$ is the Brillouin function, γ is the square root of the hole and Mn density ratio $\sqrt{p/n_i}$, $g_i(g_h)$ is Mn(hole) g

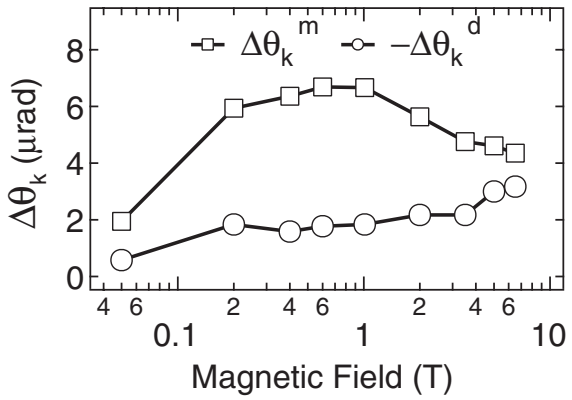

FIG. 4. Magnetic field dependence of photoinduced magnetization enhancement $\triangle\theta_k^m$ and demagnetization $\triangle\theta_k^d$ at 78 K.

factor, and S^* is given by $\sqrt{sS/(s+1)(S+1)}$. The Mn and hole spins, S and s, are $5/2$ and $1/2$, respectively. At each given $\triangle T_c$, the magnetization enhancement $\triangle M/M_0$ is solved self-consistently as a function of lattice temperature. The calculated temperature dependent $\triangle M/M_0$ and experimental $\triangle\theta_k^m$ (normalized by static θ_k at 5 K) up to 40 K are shown in the inset of Fig. 3(b) for $\triangle T_c = 1.1$ K. The results of the calculation compare well with the experimental photoenhancement peak. In addition, we can also estimate $\triangle T_c$ using an analytical expression derived from the Zener model, $\triangle T_c = \frac{1}{3} T_c \times \triangle p/p$ [18]. Knowing the ratio of photoexcited and background hole densities $\sim 2\%$, we estimate $\triangle T_c \sim 0.5$ K, in reasonable agreement with the value used in the simulation.

The photoexcited transient electrons have little effect on $\Delta\theta_K$, because of the short free electron lifetime (<1 ps) [19]. In addition, the standard thermal demagnetization via heat transfer from phonons, similar to the slow demagnetization component reported in [11,12], is also seen at temperatures below 15 K [Fig. 2(a)], which is not important to the physical picture discussed in this Letter.

Thus far our discussion has been based on a situation involving a fixed magnetic field of 1.0 T, which is important at low temperatures in order to eliminate other distractions (such as magnetization reorientation effects), without losing universality. It is worthwhile, however, to consider the field dependence of the magnetization enhancement at temperatures just above T_c and possible transient signatures of photoinduced critical phenomena, e.g., paramagnetic to ferromagnetic phase transition via the pump-induced increase of T_c. Figure 4 presents the field dependence of the magnetization enhancement $\triangle\theta_k^m$ and demagnetization $-\triangle\theta_k^d$ at 78 K. Here the most interesting aspects lie in the fact that $\triangle\theta_k^m$ is relatively constant across a wide field range (0.2–1 T) and only drops off close to zero T. It is crucial to note that, unlike static equilibrium measurements, transient pump-induced magnetization above T_c always reduces to zero at small external field, even though $\triangle T_c > 0$. A below-threshold H field is not able to activate subsequent growth of magnetic domains, even though they are nucleated via possible photoinduced long-range ferromagnetic correlation. Therefore, although the 1 K increase of $\triangle T_c$ and the substantial transient magnetization enhancement at a small field of 0.05 T suggest a transient photoinduced paramagnetic to ferromagnetic phase transition, more studies are needed to further elucidate the details of these transient features. Finally, the decrease (increase) of $\triangle\theta_k^m (-\triangle\theta_k^d)$ observed from 2 to 7 T is expected from the larger static magnetization achieved at higher fields, resulting in the smaller photoinduced changes, as indeed shown by the data.

In summary, we have observed ultrafast photoenhanced ferromagnetism in GaMnAs. Our data clearly show that the dynamic magnetization buildup occurs on a 100 ps time scale and exhibits a maximum below T_c. Our analysis and theoretical simulations, based on $H_{p\text{-}d}$ interaction between photoexcited holes and Mn spins, explain the salient features of the experimental observations, demonstrating, in particular, a correlation-induced peak below T_c and a transient increase of T_c. Our measurements thus reveal a new transient collective magnetic phenomenon, and identify the critical role of nonthermal Mn-hole exchange correlation in this photoinduced cooperative behavior. The new functionalities in subnanosecond time scales reported here may open future opportunities for high-speed spin-photon-charge integrated devices.

This work was supported by the Office of Basic Energy Sciences of the U.S. Department of Energy and by the National Science Foundation. We thank B. A. Schmid, R. A. Kaindl, and Ł. Cywiński for illuminating discussions.

[1] J. H. Harris *et al.*, Phys. Rev. Lett. **51**, 1472 (1983); D. D. Awschalom *et al.*, Phys. Rev. Lett. **55**, 1128 (1985).
[2] A. V. Kimel *et al.*, Nature (London) **429**, 850 (2004).
[3] A. V. Kimel *et al.*, Nature (London) **435**, 655 (2005).
[4] E. Beaurepaire, J.-C. Merle, A. Daunois, and J.-Y. Bigot, Phys. Rev. Lett. **76**, 4250 (1996), and references therein.
[5] S. A. McGill *et al.*, Phys. Rev. B **71**, 075117 (2005).
[6] Ganping Ju *et al.*, Phys. Rev. Lett. **93**, 197403 (2004).
[7] H. Ohno *et al.*, Phys. Rev. Lett. **68**, 2664 (1992); H. Ohno *et al.*, Appl. Phys. Lett. **69**, 363 (1996).
[8] A. H. MacDonald *et al.*, Nat. Mater. **4**, 195 (2005).
[9] S. Koshihara *et al.*, Phys. Rev. Lett. **78**, 4617 (1997).
[10] H. Ohno *et al.*, Nature (London) **408**, 944 (2000).
[11] J. Wang *et al.*, Phys. Rev. Lett. **95**, 167401 (2005).
[12] E. Kojima *et al.*, Phys. Rev. B **68**, 193203 (2003).
[13] J. Chovan *et al.*, Phys. Rev. Lett. **96**, 057402 (2006).
[14] See, e.g., *Semiconductor Spintronics and Quantum Computation* edited by D. D. Awschlom, D. Loss, and N. Samarth (Springer, Berlin, 2002).
[15] J. Wang *et al.*, J. Phys. Condens. Matter **18**, R501 (2006).
[16] B. Koopmans *et al.*, Phys. Rev. Lett. **85**, 844 (2000).
[17] S. Das Sarma *et al.*, Phys. Rev. B **67**, 155201 (2003).
[18] T. Dietl *et al.*, Science **287**, 1019 (2000).
[19] J. Wang *et al.*, Phys. Rev. B **72**, 153311 (2005).